Photoabsorption of Mg above the 3p threshold

H. S. Fung,[1] H. H. Wu,[1] T. S. Yih,[1] T. K. Fang,[2] and T. N. Chang[3]

[1]*Department of Physics, National Central University, Chung-Li, Taiwan, Republic of China 32054*

[2]*Institute of Atomic and Molecular Sciences, Academia Sinica, P.O. Box 23-166, Taipei, Taiwan, Republic of China 10764*

[3]*Department of Physics and Astronomy, University of Southern California, Los Angeles, California 90089-0484*

We present the results of a joint experimental and theoretical study on the *absolute* photoabsorption cross sections from the ground state leading to resonance structures between the Mg^+ $3p$ ^2P and Mg^+ $4s$ ^2S thresholds. The *absolute* cross sections are determined by measuring the light attenuation through a heatpipe using the synchrotron radiation. The observed spectra are compared and analyzed with the help of a *B*-spline based multichannel *K*-matrix calculation. A *hidden* $3d4p$ ^1P resonance missing from the observed spectrum is examined in detail. In addition, a nearly degenerate overlap between $3d5f$ and $4s8p$ ^1P resonances near 77.6 nm is carefully analyzed.

I. INTRODUCTION

It is well known that at an energy between the first and second ionization thresholds, the spectra of a light alkaline-earth atom are dominated by two strongly energy-dependent doubly excited asymmetric autoionization series, one broad and one narrow in width, due to the simultaneous change of electronic orbitals of two outer electrons in a double-excitation process [1,2]. In contrast, at an energy above the second ionization threshold, the width of a doubly excited resonance is usually substantially broader than the narrow resonances below the second ionization threshold, in part due to the presence of more than one ionization pathways. Moreover, the resonance profiles for the overlapping doubly excited autoionization series are expected to be less regular primarily due to the interference between transitions into multiple ionization channels.

Figure 1 shows schematically the three overlapping doubly excited autoionization series, i.e., $4snp$, $3dnp$, and $3dnf$ ^1P between the Mg^+ $3p$ ^2P and Mg^+ $4s$ ^2S thresholds. The three groups of vertical dotted lines represent the three ionization channels, i.e., $3s\epsilon p$ above the $3s$ threshold and $3p\epsilon s/3p\epsilon d$ above the 3p threshold. The theoretical calculation presented in this paper includes explicitly all three ionization channels using a recently developed *B*-spline based multichannel K-matrix (BSK) method [4]. The experiment setup and procedures leading to absolute cross section measurement are outlined in Sec. II. The physical interpretation presented in Sec. III is supported by a close agreement between theory and experiment and derived from analysis based on the BSK calculation.

II. EXPERIMENT

The instrumental setup of the photoabsorption experiment, shown schematically in Fig. 2, is similar to the one detailed in Ref. [5], except for the LiF windows that are replaced by differential pumping systems. Vacuum gauge data read from several positions along the heatpipe assure that the experimental system works as if the metal vapor is confined by a buffer gas window that has in fact kept the

heatpipe gas locked. This windowless system also keeps the monochromator along the synchrotron beam line under an optimal vacuum. The column density of the metal vapor is determined from the temperature distribution profile along the heatpipe, measured using 25 k-type thermocouples, shown in Fig. 3. A nearly constant temperature profile obtained in the present experiment has significantly reduced the uncertainty in column density. The column density nL measured in the windowless system in the present experiment is also consistent with the ones derived from the ideal gas relation by measuring simultaneously the temperature profile and the total pressure in the heatpipe furnace with a LiF window at a longer wavelength from previous experiments [5,6]. Our estimated total uncertainty for the windowless system is about 25%, which is noticeably worse than the 13% for the window system. However, it still compares favorably to a typical 30% estimated error for spectra in other earlier
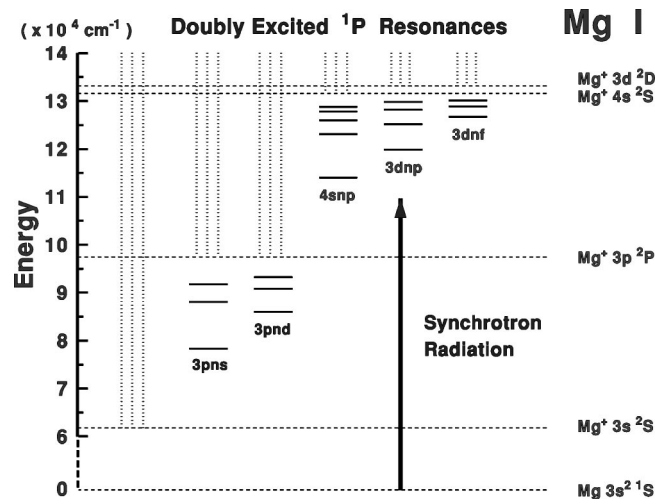

FIG. 1. Energy diagram for one photon photoabsorption from the ground state of Mg to the doubly excited ^1P resonances. The vertical dotted lines represent the continua above their respective ionization thresholds. The Mg^+ $3p$ ^2P and Mg^+ $4s$ ^2S thresholds are 102.7 nm and 76.06 nm, respectively, above the Mg ground state [3].
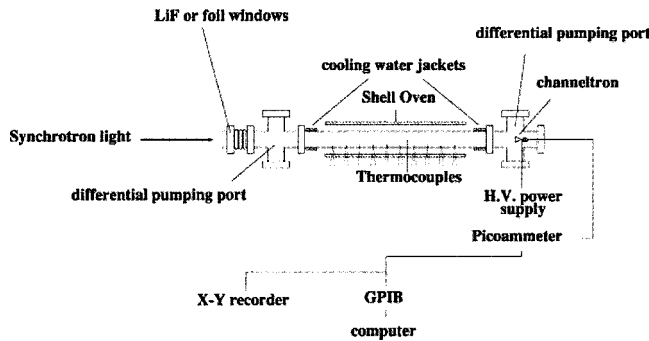
FIG. 2. Schematic diagram of the experimental setup. The system is similar to the one shown by Fig. 1 in Ref. [5], except for the LiF windows that are replaced by differential pumping systems in the present experiment.

measurements using the quoted metal vapor density data.

The synchrotron radiation source at Synchrotron Radiation Research Center (SRRC) in Hsinchu, Taiwan is employed as the continuum background. The transmitted light was detected by a channeltron shown in Fig. 2. The estimated spectral bandwidth of the monochromator was 0.08 nm. The absolute photoabsorption cross section $\sigma(\lambda)$ at a wavelength λ is determined using the Beer-Lambert law

$$I(\lambda) = I_0(\lambda) e^{-\sigma(\lambda)nL}, \qquad (1)$$

where I_0 is the intensity of the incident light, $I(\lambda)$ is the attenuated intensity of the transmitted light, n is the number density, and L is the effective interaction length. In the present experiment, the absolute value of $\sigma(\lambda)$ is measured by replacing nL with $\Sigma_{i=1}^{25} n_i L_i$ in Eq. (1) to reduce the uncertainty introduced by the use of an estimated effective length. The cross section σ is evaluated from the slope in the region where $ln(I_0/I)$ varies linearly against nL.

III. RESULTS AND DISCUSSION

All three doubly excited autoionization series, i.e., $4snp$, $3dnp$, and $3dnf$ ^1P shown schematically in Fig. 1, are identified explicitly from the BSK calculation. The theoretical energy E_t is calculated against the Mg double-ionization
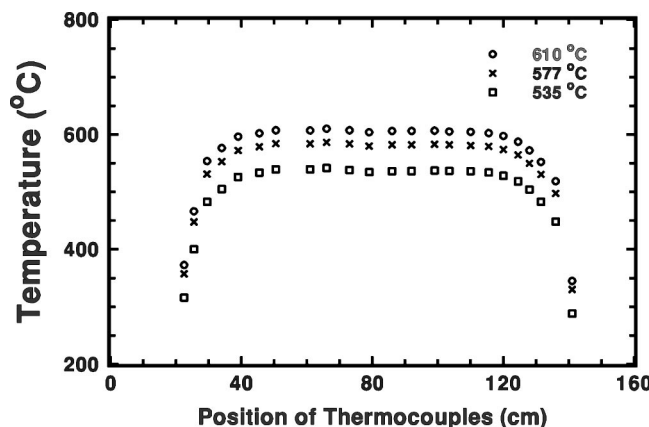

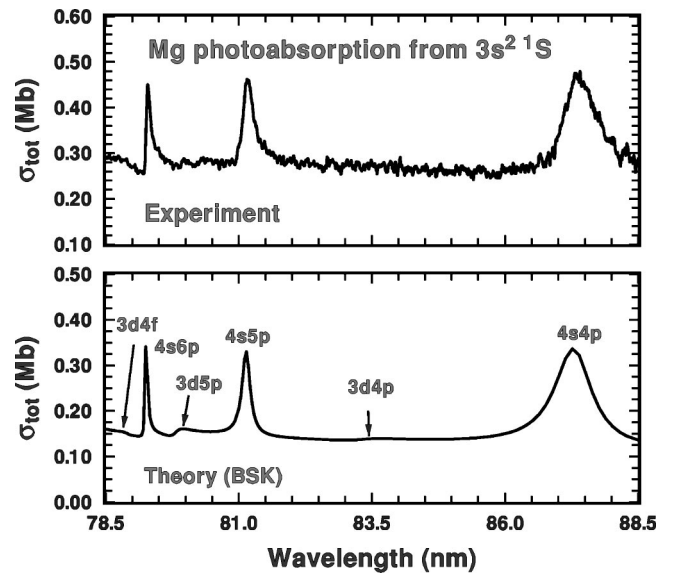FIG. 3. A typical temperature distribution profile in the heatpipe.

FIG. 4. Comparison between measured absolute photoabsorption cross sections and theoretical photoionization cross sections using BSK approach from 78.5 nm to 88.5 nm.

threshold at $E_{II} = 182\,938.63$ cm^{-1} above the Mg ground state [3]. Accordingly, the theoretical photon energy is given by $E_p = E_{II} - |E_t|$. Our BSK results are quantitatively consistent with an earlier L^2-based configuration interaction calculation by Mengali and Moccia [7]. It also agrees qualitatively
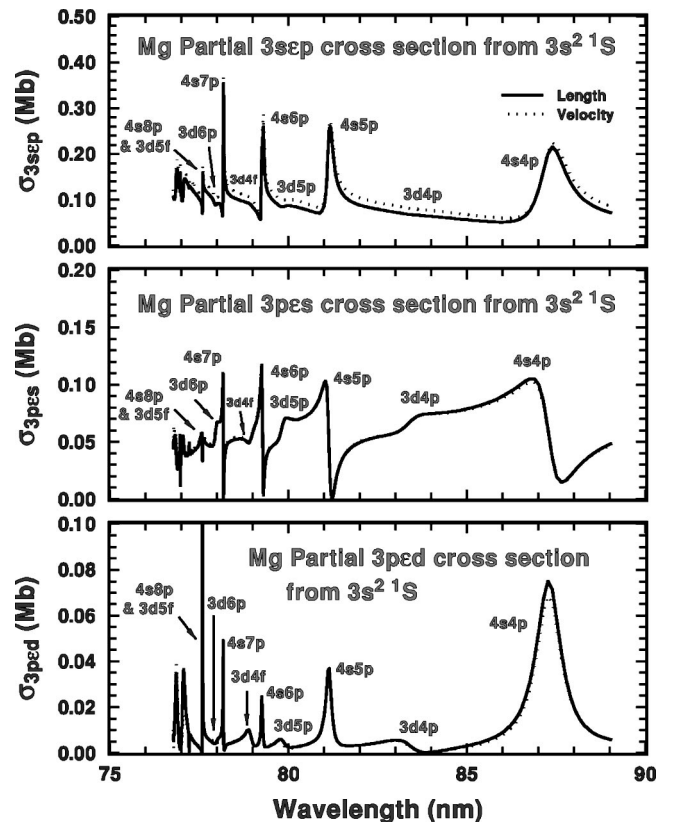

FIG. 5. Theoretical partial photoionization cross sections from the $3s^2$ ^1S ground state of Mg above the $3p$ threshold.
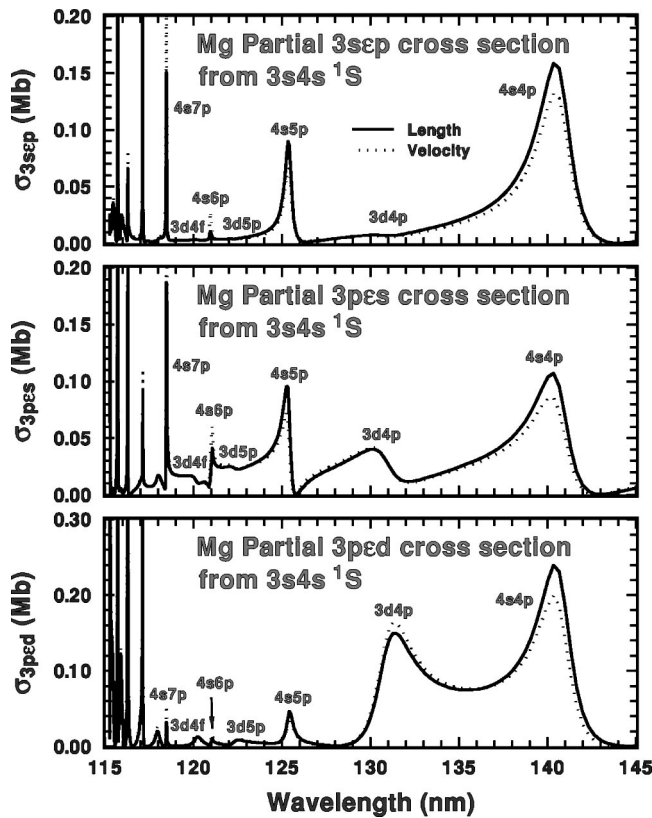
FIG. 6. Theoretical partial photoionization cross sections from the $3s4s\ ^1S$ bound excited state of Mg above the $3p$ threshold. The wavelength is converted from the photon energy measured against the Mg $3s4s\ ^1S$ state at 43 503.33 cm^{-1} above the ground state [3].

with the result of a close-coupling calculation by Butler *et al.* [8]. Our observed resonance energies agree with the data derived from the photoabsorption spectrum of Baig and Conerade [9] up to about 77 nm before they lost the details due to a strongly absorbing continuum in the background. The
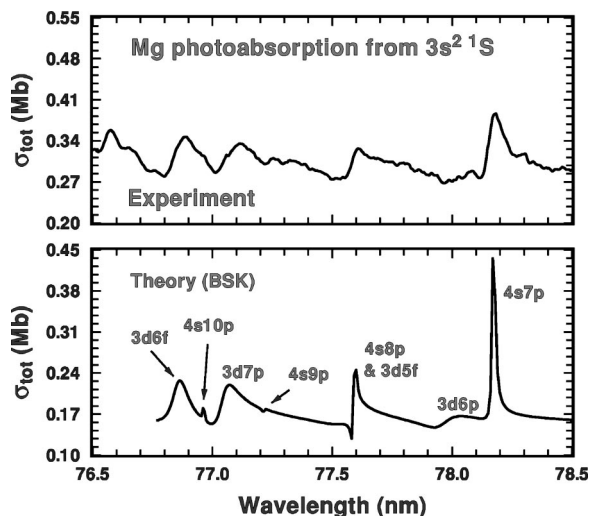

FIG. 7. Comparison between measured absolute photoabsorption cross sections and theoretical photoionization cross sections using BSK approach from 76.5 nm to 78.5 nm.
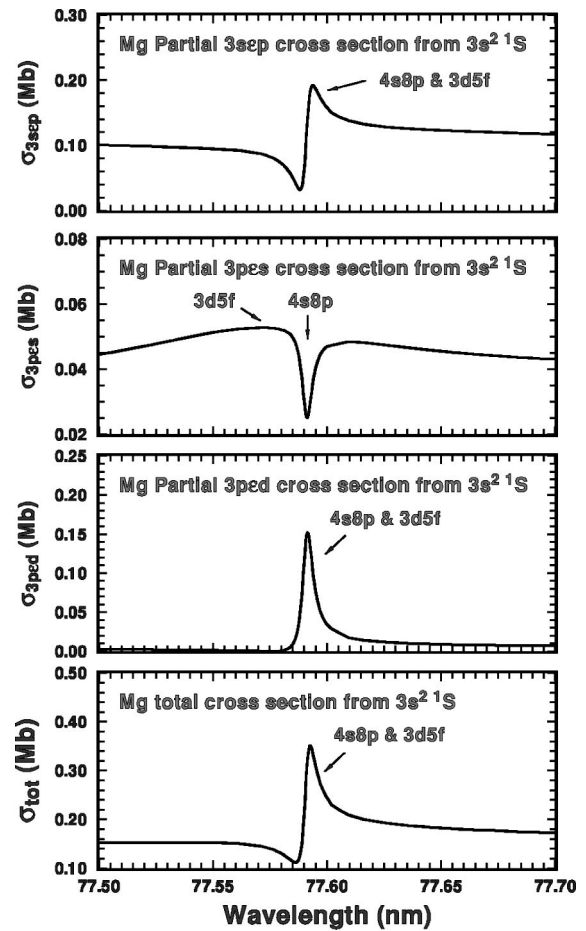

FIG. 8. The overlapping narrow $4s8p\ ^1P$ resonance and the broad $3d5f\ ^1P$ resonance near 77.6 nm.

overall agreement between BSK results and our observed absolute photoabsorption spectrum in terms of the resonance energy and the spectral profile is very good. The only disagreement between theory and experiment is an approximate 0.1 Mb difference in the absolute cross section over the entire spectral region.

Figure 4 compares our measured photoabsorption cross sections from the ground state of Mg above the Mg$^+$ $3p\ ^2P$ threshold between 78.5 nm to 88.5 nm with the calculated photoionization result using the BSK approach. One of the more interesting features is a *hidden* $3d4p\ ^1P$ resonance near 83.5 nm. Its presence, visually missing both in theoretical and experimental total cross section spectra, is seen clearly in the theoretical partial cross section spectra at least in two of the ionization channels (i.e., $3p\epsilon s$ and $3p\epsilon d\ ^1P$) shown in Fig. 5. In addition, the BSK calculation shows clearly that, if the photoionization is originated from the bound excited $3s4s\ ^1S$ state, the $3d4p\ ^1P$ resonance can be seen unambiguously in all partial ionization spectra shown in Fig. 6.

Figure 7 compares our observed and calculated spectra at wavelengths shorter than 78.5 nm. The calculated structure profiles shown are not convoluted. Clearly, the individual resonant features along the same autoionization series are not as regular as those at lower energy or below the second ion-
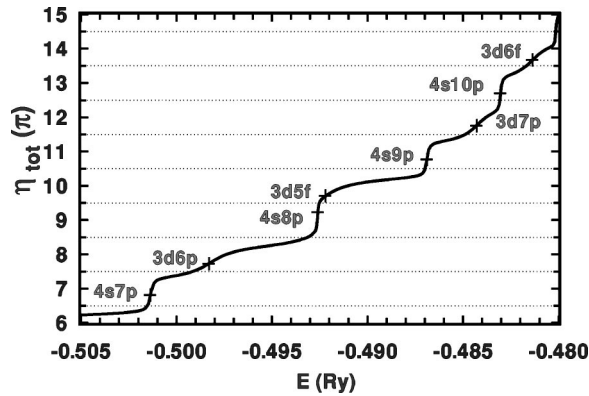
FIG. 9. Energy variation of η_{tot}. (E in Ry is measured relative to the Mg^{+2} threshold.)

ization threshold. In particular, a simple calculation of the effective principal quantum numbers of the $4s\nu p$ and $3d\nu f$ series against the $4s$ and $3d$ thresholds, respectively, suggests that at an energy close to 77.6 nm, there should exist one member from each of these two autoionization series. However, neither spectrum shown in Fig. 7, with only one asymmetric resonance structure visible near 77.6 nm, supports the presence of two overlapping resonances. A detailed analysis based on the theoretical calculation confirms a nearly degenerate overlap between a broad $3d5f$ and a narrow $4s8p$ resonances near 77.6 nm. In fact, Fig. 8 shows that a narrow $4s8p$ resonance can be easily identified from the $3p\epsilon s$ partial cross-section spectrum. This narrow resonance is located near the center of a broad $3d5f$ resonance, leading to an appearance of a single resonance in the total cross section.

Alternatively, the overlapping of these two resonances can also be analyzed by examining the energy variation of the sum of the eigenphase shifts over all eigenchannels, η_{tot}. Similar to the energy variation of the scattering phase shifts across a doubly excited resonance in a single-channel ionization, η_{tot} is also expected to increase by a total of π across a resonance in a multichannel ionization (see, e.g., Eq. (16) of Ref. [4]). Figure 9 shows that unlike the increase in η_{tot} a value of π for all other resonances, an increase of a value close to 2π in η_{tot} between $E=-0.496$ Ry and -0.489 Ry (i.e., at wavelengths centered around 77.6 nm), confirms the presence of the overlapping $3d5f$ and $4s8p$ resonances suggested by the theoretical partial cross section spectra shown in Fig. 8. Finally, we list in Table I the resonant energies E_r and the resonant widths Γ of a number of selected resonances derived from the calculated energy variation of η_{tot}. The results from the BSK calculation are generally in good agreement with other existing theoretical calculations and experimental data.

TABLE I. The resonant energy E_r (upper entry in a.u.) measured against the Mg III ground-state energy and the widths Γ (lower entry in $a[n]=a\times10^n$ a.u.) of selected Mg $4s\mu p$, $3d\mu p$, and $3d\mu f$ ^1P resonances.

		Theory			Experiment	
State	Present	Ref. [7]	Ref. [10]	Ref. [11]	Ref. [9]	
$4s4p$ ^1P	−0.3116	−0.3126	−0.3124	−0.3117	−0.3125	
	5.01[−3]	4.3[−3]				
$3d4p$ ^1P	−0.2870	−0.2877				
	5.90[−3]	5.5[−3]				
$4s5p$ ^1P	−0.2720	−0.2725	−0.2716	−0.2727	−0.2733	
	1.27[−3]	1.3[−3]				
$3d5p$ ^1P	−0.2627	−0.2629				
	2.06[−3]	1.9[−3]				
$4s6p$ ^1P	−0.2587	−0.2590	−0.2587	−0.2580	−0.2597	
	2.57[−4]	2.6[−4]				
$3d4f$ ^1P	−0.2562	−0.2561				
	1.51[−3]	1.3[−3]				
$4s7p$ ^1P	−0.2507	−0.2511	−0.2507	−0.2518	−0.2515	
	9.88[−5]	1.1[−4]				
$3d6p$ ^1P	−0.2492	−0.2492				
	9.94[−4]	9.4[−4]				
$4s8p$ ^1P	−0.2463	−0.2468	−0.2459	−0.2473	−0.2461	
	3.93[−5]	2.1[−5]				
$3d5f$ ^1P	−0.2462	−0.2460				
	1.11[−3]	8.8[−4]				
$4s9p$ ^1P	−0.2434	−0.2439		−0.2451	−0.2432	
	7.71[−5]					
$3d7p$ ^1P	−0.2421	−0.2423				
	5.53[−4]	5.6[−4]				
$4s10p$ ^1P	−0.2415					
	4.47[−5]					
$3d6f$ ^1P	−0.2407					
	5.33[−4]					

In conclusion, a joint theoretical and experimental study, such as the one presented in this paper, offers the possibility of a detailed interpretation of the resonant structures of overlapping autoionization series, including those features that may be *hidden* otherwise, in a spectral region that is substantially affected by the interchannel interaction for transitions involving multiple ionization pathways.

ACKNOWLEDGMENTS

[1] J.M. Esteva, G. Mehlman-Balloffet, and J. Romand, J. Quant. Spectrosc. Radiat. Transf. **12**, 1291 (1972); G. Mehlman-Balloffet and J.M. Esteva, Astrophys. J. **157**, 945 (1969); J.P. Preses, C.E. Burkhardt, W.P. Garver, and J.J. Leventhal, Phys. Rev. A **29**, 985 (1984); W. Fiedler, Ch. Kortenkamp, and P. Zimmermann, *ibid.* **36**, 384 (1987).

[2] G.N. Bates and P.L. Altick, J. Phys. B **6**, 653 (1973); C. Froese Fischer and H.P. Saha, Can. J. Phys. **65**, 772 (1987); R. Moccia and P. Spizzo, J. Phys. B **21**, 1145 (1988); R. Moccia and P. Spizzo, Phys. Rev. A **39**, 3855 (1989); T.N. Chang, in *Many-body Theory of Atomic Structure and Photoionization*, edited by T. N. Chang (World Scientific, Singapore, 1993), p. 213.

[3] W.C. Martin and R. Zalubas, J. Phys. Chem. Ref. Data **9**, 1 (1980).

[4] T.K. Fang and T.N. Chang, Phys. Rev. A **61**, 062704 (2000).

[5] C.C. Chu, H.S. Fung, H.H. Wu, and T.S. Yih, J. Phys. B **31**, 3843 (1998).

[6] H.S. Fung, C.C. Chu, S.J. Hsu, H.H. Wu, and T.S. Yih, Rev. Sci. Instrum. **71**, 1564 (2000).

[7] S. Mengali and R. Moccia, J. Phys. B **29**, 1597 (1996); **29**, 1613 (1996).

[8] K. Butler, C. Mendoza, and C.J. Zeippen, J. Phys. B **26**, 4409 (1993).

[9] M.A. Baig and J.P. Connerade, Proc. R. Soc. London **364**, 353 (1978).

[10] V.I. Lengyel, V.T. Navrotsky, E.F. Sabad, and O.I. Zatsarinny, J. Phys. B **17**, L465 (1984).

[11] V. Pejcev, D. Rassi, and K.J. Ross, J. Phys. B **13**, L305 (1980).